Sensors and Materials, Vol. 36, No. 12 (2024) 5395–5410
MYU Tokyo

S & M 3875

Bridge Pier Verticality Detection Considering Surface Point Cloud Curvature Characteristics

Xianglei Liu,[1] Di Cai,[1] and Runjie Wang[1,2*]

[1]Key Laboratory for Urban Geomatics of National Administration of Surveying,
School of Geomatics and Urban Spatial Informatics, Beijing University of Civil Engineering and Architecture,
No. 1, Zhanlanguan Road, Beijing 100048, PR China
[2]Beijing Key Laboratory of Urban Spatial Information Engineering,
No. 15, Yangfangdian Road, Beijing 100038, PR China

(Received February 16, 2024; accepted May 2, 2024)

Keywords: TLS, bridge pier verticality, interpolation-matrix method, shadow texture area

Bridges are vital transportation infrastructure in our country, with bridge piers being a critical component. Damage to bridge piers can pose significant safety hazards, potentially leading to bridge collapse. Verticality serves as a crucial indicator for assessing pier damage. In this study, we employed terrestrial 3D laser point clouds to evaluate bridge pier verticality. However, owing to curvature features on pier surfaces, the point clouds exhibit nonuniformity. Moreover, external factors such as collisions contribute to the presence of shadowed texture area on the pier surfaces. Therefore, in this paper, we propose the use of (1) interpolation-matrix transformation for point cloud surface curvature calculation, in order to solve the problem of low curvature calculation accuracy caused by the nonuniform distribution of the point clouds. (2) Shadow texture area identification and removal are achieved through changes in curvature features, aiming to enhance the bridge pier verticality change detection accuracy. (3) The verticality of the bridge piers is computed and monitoring procedures are established for detecting changes. Experimental results showed that the proposed method can detect bridge pier verticality.

1. Introduction

With urban transportation development, bridges are becoming increasingly important in urban transportation routes. Bridge piers are an important part of a bridge. Pier damage can lead to serious safety hazards in maintaining a bridge's safe operation.[1,2] Verticality is one of the most important indicators that can reflect the status of bridge piers.[3] Therefore, the accurate and rapid detection of bridge pier verticality changes is important for maintaining the safe operation of bridges.

Currently, the most commonly used method for detecting changes in bridge pier verticality is the traditional periodic inspection through the total station, bridge trucks, and so forth.[4] The above method can accurately show changes in bridge pier verticality. However, for detecting

*Corresponding author: e-mail: wangrunjie@bucea.edu.cn
https://doi.org/10.18494/SAM5025

ISSN 0914-4935

such changes, it has low efficiency and is expensive. Moreover, the overall bridge pier verticality cannot be completely detected, which affects the integrity of bridge pier verticality calculation.(5) In recent years, terrestrial 3D laser scanners (TLSs) have been widely used in bridge damage detection.(6) The TLS method offers a higher efficiency than traditional methods for obtaining bridge pier point clouds. It allows for bridge pier comprehensive scanning in a shorter period. This reduces the prolonged outdoor work required by traditional inspection methods. Additionally, it can capture the 3D information of the bridge pier comprehensively, including every detail and feature on the surface. There is no risk of omission due to operator subjective factors. It can also realize the accurate acquisition of pier verticality columns and detect the change in pier verticality as a whole, in order to judge the bridge pier damage state.

Accurate bridge pier verticality detection is important for determining the damage status.(7) However, during a bridge's daily operation, bridge piers may develop notches on the surface due to collisions, erosion, and other reasons. These notches can lead to missing parts in the bridge pier physical model. They can also lead to shadow texture areas in the bridge pier surface point cloud. The shadow texture areas can affect the verticality change detection accuracy. For clarity, a cylindrical bridge pier is taken as an example. The ideal bridge pier point cloud model is shown in Fig. 1(a). The bridge pier is a standard cylinder, in which vertical lines completely represent pier verticality. As shown in Fig. 1(b), when the bridge pier surface has a shaded texture area, the center plumbline will be offset owing to the fitted residual surface. The offset center plumb line will affect the bridge pier damage determination accuracy.

Therefore, there is a need to identify and process the shadow texture area. To accurately identify the shaded texture area, the bridge pier surface needs to be accurately described. Currently, features that provide the bridge pier surface an accurate description include gradient and curvature.(8) Gradient is primarily used to detect the local and edge features of point clouds, rather than capturing the entire surface texture information. Since bridge pier surfaces are typically continuous curves containing rich texture information, it is difficult to use gradient in accurately capturing the entire bridge pier surface texture information. Additionally, bridge pier

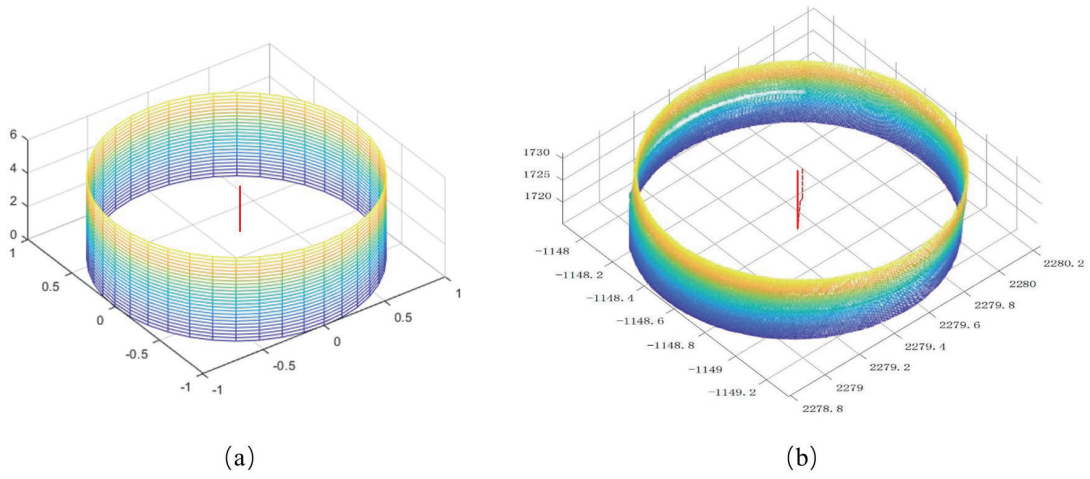

(a) (b)

Fig. 1. (Color online) (a) Bridge pier in the ideal state and (b) bridge pier with the shaded texture.

surfaces may exhibit various types of damage. This can lead to complex changes in surface shape and texture. Because the use of gradient primarily focuses on local and edge features, it cannot effectively distinguish these complex damage types and accurately capture the texture changes.[9] Curvature is an important feature for expressing the smooth morphology of point clouds.[10] Curvature characteristics remain unchanged if the surface is smooth. If there is a shadow texture area on the surface, the point cloud curvature will change abruptly. Morgenthal *et al.* obtained the point cloud data of a glass bridge to identify different crack damage degrees, including the number of cracks and curvatures of different cracking positions.[11] The obtained damage position results were the same as the actual ones. Aryal *et al.* acquired the discrete point cloud data on the surface of a cracked box girder model using a TLS.[12] A sudden curvature change was found on the deformed place. Therefore, curvature can effectively identify the shadow texture of the damaged area on the outer surface by calculating the point cloud curvature of the bridge pier outer surface and determine damage degree according to the change in curvature. Thus, processing the bridge pier point cloud shadow texture area can improve the verticality calculation accuracy.

The bridge pier point clouds based on a TLS are mostly uniformly distributed in an arc shape owing to the existence of curvature in the pier morphology.[13] When collecting bridge pier point clouds, there will be a nonuniform distribution that is dense in the middle and sparse on both sides. It reduces the curvature calculation accuracy of the bridge pier outer surface.[14] To address this inaccuracy problem, we propose an interpolation-matrix transformation method in this paper. The traditional matrix transformation method unfolds the point cloud through the form of matrix transformation.[15] The unfolded point cloud is more intuitive and efficient than the stereo point cloud in the curvature calculation in the 2D point cloud coordinate system.[16] By calculating the point cloud curvature, the bridge pier outer surface curvature information can be obtained more easily. On the basis of the matrix transformation method, the fusion interpolation method interpolates the point cloud in the nonuniform point cloud region on the bridge pier outer surface, so as to homogenize the bridge pier point cloud.[17] After the bridge pier point cloud is homogenized and its curvature is calculated, the curvature of the point cloud will change abruptly in the shadow texture area.[18] Although interpolation and matrix transformation methods can address certain aspects of the problem separately, the interpolation method can lead to excessive smoothing or distortion when point cloud data is sparse, and the matrix transformation method cannot effectively alleviate the impact of nonuniformity. Therefore, combining them can effectively enhance the accuracy of curvature calculation results. The interpolation method can fill in sparse areas, increasing the density and smoothness of the point cloud. Thus, it can provide a more uniform data input for the matrix transformation method. The latter method can globally transform point cloud data, thereby mitigating the effects of nonuniformity and making the point cloud more suitable for the interpolation method. If there is a shadow texture area on the bridge pier surface, the point cloud coordinates of the abnormal curvature position are eliminated. Then, we can improve the accuracy of bridge pier verticality detection.[19] After homogenizing the bridge pier point cloud and calculating its curvature, abrupt changes in curvature may occur in the bridge pier surface shadow texture area.[20] By eliminating the area where the point cloud abrupt curvature changes, the effect of the shadow

texture area can be mitigated, thereby improving the accuracy of bridge pier verticality detection.

To sum up, in order to detect the bridge pier verticality accurately, we propose in this paper an innovative method that considers point cloud surface curvature characteristics and mainly includes the following three key components: (1) Interpolation-matrix transformation is used for point cloud surface curvature calculation, in order to solve the problem of low curvature calculation accuracy caused by the nonuniform distribution of point clouds. (2) Shadow texture area identification and removal are achieved through changes in curvature features, aiming to enhance the accuracy of bridge pier verticality change detection. (3) The verticality of the bridge piers is calculated and monitoring procedures for detecting changes are established. The rest of the paper is organized as follows. In Sect. 2, we describe the methodology used. In Sect. 3, we show the experimental results and analysis. Conclusions are given in Sect. 4.

2. Methods

Figure 2 shows the technical flow of the proposed method for calculating the bridge pier verticality, including three steps: (1) interpolation-matrix transformation for bridge pier surface curvature calculation, (2) bridge pier surface shadow identification and processing, and (3) bridge pier verticality calculation and bridge pier damage level assessment.

2.1 Interpolation-matrix transformation method for homogenized bridge pier point cloud

As shown in Fig. 3, when the TLS method is performed, a point cloud will be dense in the middle and sparse on both sides. This complex nonuniform distribution of the bridge pier point

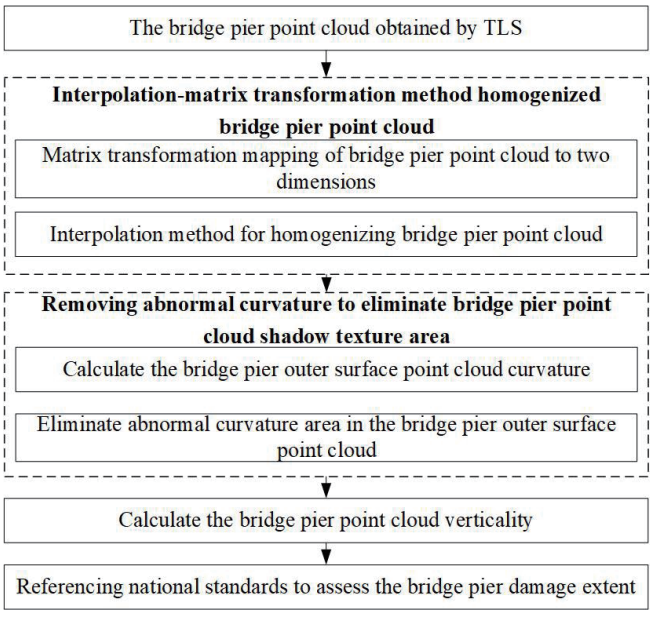

Fig. 2. Overall flowchart for bridge pier verticality.

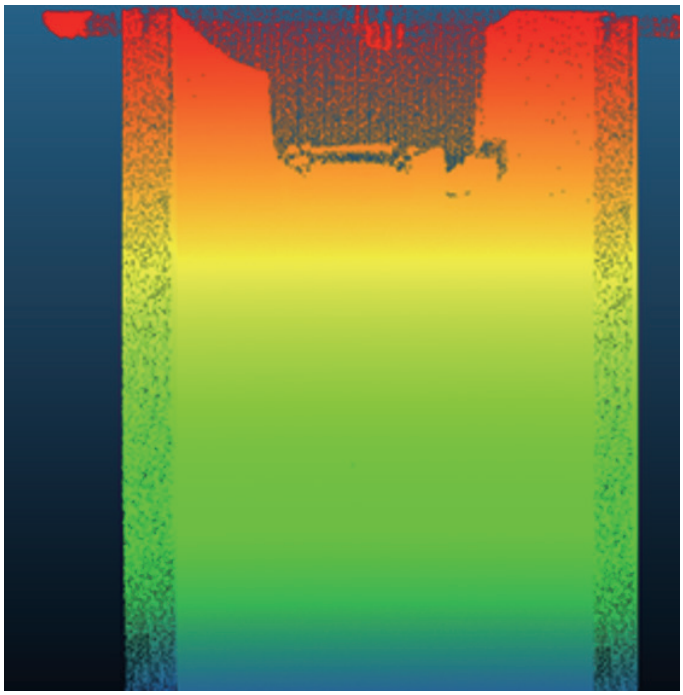

Fig. 3. (Color online) Beishatan bridge pier nonuniform point cloud.

cloud will lead to inconsistency in the point number in the neighboring range when calculating the curvature,[21] which will reduce the accuracy of point cloud curvature calculation.

To eliminate this nonuniform point cloud situation and improve the accuracy of calculating the bridge pier point cloud curvature, we propose an interpolation-matrix transformation method in this paper.

First, the 3D coordinates of the point $P=(x,y,z)$ and their column-vector representation are as follows.

$$P=\begin{bmatrix} x \\ y \\ z \end{bmatrix} \tag{1}$$

Here, x, y, and z represent the three coordinates of a point.

The mapping of a 3D point cloud into 2D is represented by a transformation matrix that includes translation, rotation, scaling, and other transformation parameters, which are uniformly distributed on the 2D plane.[22]

$$P'=\begin{bmatrix} x \\ y \\ z \end{bmatrix} * \begin{bmatrix} a & b & c & d \\ e & f & g & h \\ i & j & k & l \\ 0 & 0 & 0 & 1 \end{bmatrix} \tag{2}$$

Here, P' represents the new coordinates after mapping to the 2D plane.

After mapping to 2D, interpolation is performed on the nonuniform point cloud by setting a threshold interpolation to eliminate the problem of low accuracy of curvature calculation for nonuniform piers due to the curvature feature.

$$Delta\_Points(x, y) = D\_target - D(x, y) \tag{3}$$

D_target represents the target value, which is used as the basis for interpolation at that position in point cloud coordinates.

Threshold interpolation is applied to interpolate the nonuniform point cloud caused by curvature features on the bridge pier surface, thereby improving the overall accuracy of curvature calculation. Setting a threshold for interpolation addresses the issue of the low accuracy of curvature calculation for nonuniform bridge piers.

2.2 Elimination of bridge pier point cloud shadow texture area

On the bridge pier point cloud surface, the shadow texture area may appear owing to collision or erosion,[23] as shown in Fig. 4(a). The shadow texture area can cause gaps in establishing the bridge pier point cloud model. The shape of the bridge pier point cloud gap can lead to abnormal offsets in verticality calculations, as shown in Fig. 4(b).

Shadow texture areas can result in gaps when calculating the bridge pier verticality. The computation of verticality may exhibit specific anomalies in the shadow texture area.[24] Therefore, to identify and eliminate the shadow texture area, curvature is introduced. The curvature of the bridge pier surface point cloud is calculated, and the positions with abnormal curvature correspond to the shadow texture area. The traditional method suffers from the low accuracy of the computational results for normal vectors with diverging directions. Therefore, we introduce the unit normal vector of the point cloud, normalize it, and construct the curvature of the bridge using the proposed normal vector normalization constraint coordinate transformation method. In this way, the divergence phenomenon of the point cloud surface normal direction can be suppressed. It can improve the accuracy of the curvature results. The flow of calculating the curvature is as follows.

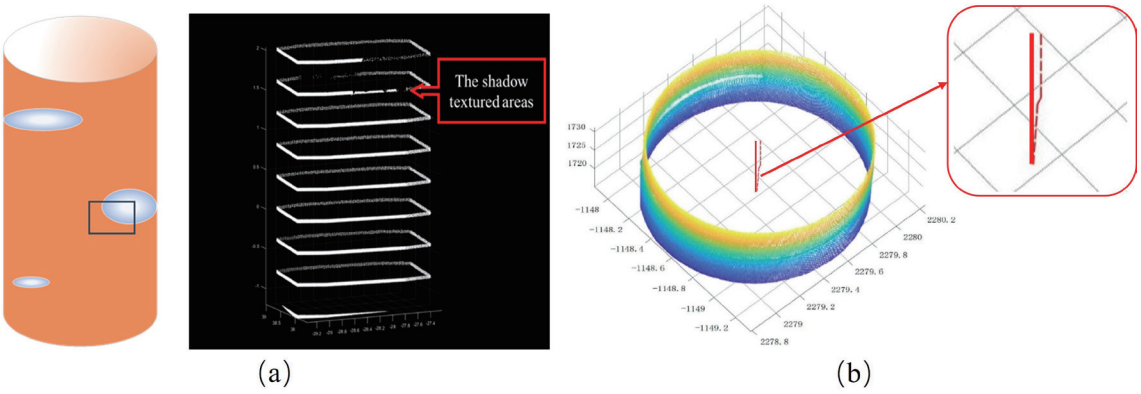

Fig. 4. (Color online) (a) Bridge pier point cloud shadow texture area. (b) Verticality offset.

(1) After applying the fusion interpolation-matrix transformation method, the bridge pier from the stereo point cloud into a planar point cloud, the rectangle is defined as the plane $r = r(x, y) = (x, y, z(x, y))$ in the calculation of the curvature of the point cloud before the need to calculate the point cloud normal vector.

$$r_x = \left(1, 0, \frac{\partial z}{\partial x}\right) \tag{4}$$

$$r_y = \left(0, 1, \frac{\partial z}{\partial y}\right) \tag{5}$$

The unit normal vector is as follows.

$$\vec{n} = \frac{r_x \times r_y}{\left|r_x \times r_y\right|} = \frac{\left(-\frac{\partial z}{\partial x}, -\frac{\partial z}{\partial y}, 1\right)}{\sqrt{1 + \left(\frac{\partial z}{\partial x}\right)^2 + \left(\frac{\partial z}{\partial y}\right)^2}} \tag{6}$$

(2) The first fundamental E, F, G and second fundamental L, M, N forms of the rectangular plane of the point cloud can be calculated from the unit normal vector.

$$E = \frac{\partial r}{\partial x} \cdot \frac{\partial r}{\partial x} \tag{7}$$

$$F = \frac{\partial r}{\partial x} \cdot \frac{\partial r}{\partial y} \tag{8}$$

$$G = \frac{\partial r}{\partial y} \cdot \frac{\partial r}{\partial y} \tag{9}$$

$$L = \vec{n} \cdot \vec{r}_{xx} = \frac{z_{xx}}{\sqrt{1 + z_x^2 + z_y^2}} \tag{10}$$

$$M = \vec{n} \cdot \vec{r}_{xy} = \frac{z_{xy}}{\sqrt{1 + z_x^2 + z_y^2}} \tag{11}$$

$$N = \vec{n} \cdot \vec{r}_{yy} = \frac{z_{yy}}{\sqrt{1 + z_x^2 + z_y^2}} \tag{12}$$

Included among these are $\vec{r}_{xx}=\frac{\partial^2 S}{\partial x^2}$, $\vec{r}_{xy}=\frac{\partial^2 S}{\partial x\partial y}$, $\vec{r}_{yy}=\frac{\partial^2 S}{\partial y^2}$, $z_{xx}=\frac{\partial^2 \mathrm{z}}{\partial x^2}$, $z_{xy}=\frac{\partial^2 \mathrm{z}}{\partial x\partial y}$, $z_{yy}=\frac{\partial^2 z}{\partial y^2}$, $z_x=\frac{\partial z}{\partial x}$, and $z_y=\frac{\partial z}{\partial y}$.

By using the first and second fundamental forms of the above calculation, the point cloud curvature can be calculated as

$$K=\frac{LN-M^2}{EG-F^2}. \tag{13}$$

2.3 Bridge pier verticality calculation and damage judgement

Verticality represents the alignment of the bridge pier relative to the vertical direction, indicating whether the bridge pier is perpendicular to the ground.[25] In this work, the slicing method, which is shown in Fig. 5, is used to calculate the bridge pier verticality.

In the selected slices, $\overline{Z_u}$ and $\overline{Z_d}$ $\Delta=K\rho\approx\overline{Z_u}-\overline{Z_d}\,(K>0)$. $\overline{Z_u}$ and $\overline{Z_d}$ show the average of the point cloud Z-coordinate values of the selected slices and the thickness of each slice, respectively. The coordinate values are denoted by $\overline{Z_u}+\frac{K\rho}{2}$.

To eliminate the impact of the shadow texture area on the calculation of bridge pier verticality, the slicing method can be employed. The number and density of slices can be adjusted as needed to remove the sections of abnormal curvature in the bridge pier, thereby improving the accuracy of verticality detection.

After the selection of slices, perpendicularity is calculated by least squares fitting as shown below.

The fitting equation is $f(x,y)=x^2+ax+y^2+\beta y+\delta=0$. The coordinates of the center points can be calculated from the bridge pier point cloud slices fitted by the least squares method.

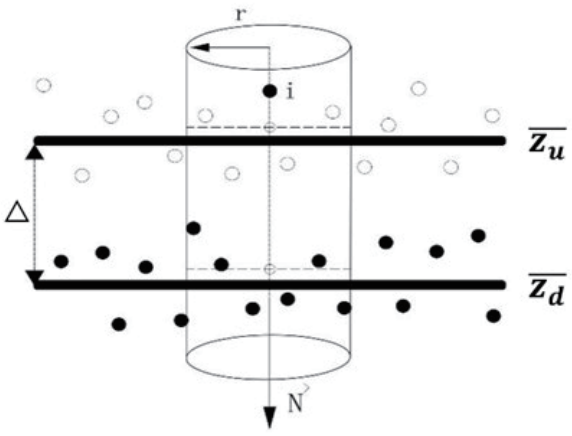

Fig. 5. Slice selection by slicing method.

The coordinates of the center of the circle are $(-\alpha/2, -\beta/2)$, and the radius is $r = \sqrt{\frac{\alpha^2 + \beta^2 - 4\delta}{2}}$ in Fig. 6.

After fitting each slice, we calculate the coordinates of the center point. Connecting the lines formed by these center point coordinates represents the bridge pier verticality. Assuming that the number of slices per column is j, the center of the fitted circle for each slice of a single column has a coordinate value in the spatial coordinate system.

$$\left(-\frac{\alpha}{2}, -\frac{\beta}{a}, \overline{Z_{uj}} + \frac{K\rho}{2}\right), j = 1, 2, 3, ..., m \tag{14}$$

The column axis $\vec{P}$ is fitted according to the spatial coordinate points. Its angle θ with $N(0,0,1)$ is calculated using the equation

$$i = \cos\left(\frac{\vec{P} \cdot \vec{N}}{|\vec{P}| \cdot |\vec{N}|}\right) = \frac{P_x N_x + P_y N_y + P_z N_z}{\sqrt{P_x^2 + P_y^2 + P_z^2} \cdot \sqrt{N_x^2 + N_y^2 + N_z^2}}, \tag{15}$$

where i is the bridge pier verticality. Bridge pier damage assessment can be determined according to national standards. Currently, according to national standards, the offset of the bridge pier verticality should not exceed 0.02% of the bridge height.

3. Experiment

3.1 Overview of experimental area

In this study, a damaged urban bridge, Beishatan Bridge, was selected as the experimental bridge. Beishatan Bridge is a representative of small- and medium-sized cross-border bridges. This bridge is selected for study as it is currently in a state of imminent damage and has been

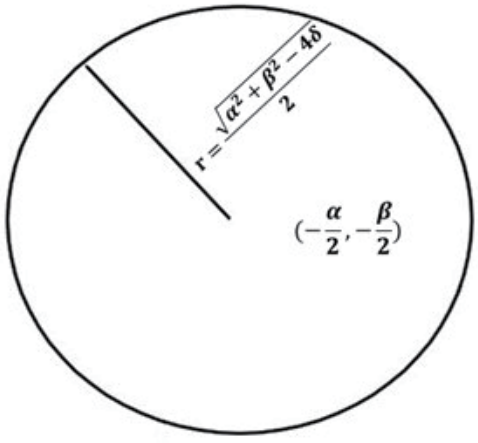

Fig. 6. Least squares fitting schematic.

properly maintained by the state. It is located between the North Fourth Ring and the North Fifth Ring in Beijing, and it is an important route connected to the G6 motorway. Beishatan Bridge is composed of a right sub-bridge (direction toward Beijing) and a left sub-bridge (direction away from Beijing). Both sub-bridges have the same length and width. Each sub-bridge is an 86.58 m continuous girder bridge divided into three spans: a main span of 40 m and two side spans of 19.6 and 26.98 m. Moreover, as shown in Fig. 7, the right sub-bridge of Beishatan Bridge has been damaged to a greater extent than the left sub-bridge. It is now supported by jacks to avoid further deterioration.

In this study, the TLS Riegl VZ-1000 was used to collect the point cloud of the Beishatan bridge pier, as shown in Fig. 8(a). With high-density point cloud data acquisition, the instrument can measure up to 1400 m. It has a laser emission frequency of 300000 dots/s and a scanning accuracy of 5 mm (100 m distance, single-point scanning). In addition, the Riegel VZ-1000 has a field of view scanning range of 100° * 360° (vertical * horizontal). Although it is a low- to medium-resolution TLS, the Riegel VZ-1000 is highly scalable and practical for real-world engineering needs. At present, Riegl scanners meet actual engineering requirements. Although they have a low resolution, Riegl scanners have a high degree of applicability.

As shown in Fig. 8(b), during the point cloud data acquisition, the buildings or noises around the measured object will produce a large amount of surrounding noise in the point cloud. Therefore, we are the first to perform the noise reduction process for the collected point cloud data, and the results are shown in Fig. 8(c).

3.2 Interpolation-matrix transformation method for homogenized bridge pier point cloud

Owing to the curvature features on the bridge pier surface, the point cloud on the bridge pier surface becomes nonuniform, as shown in Fig. 9(a). The nonuniform point cloud can lead to a decrease in accuracy when calculating the curvature of the bridge pier's outer surface point cloud. To homogenize the nonuniform point cloud, we introduce the interpolation-matrix transformation method in this paper.

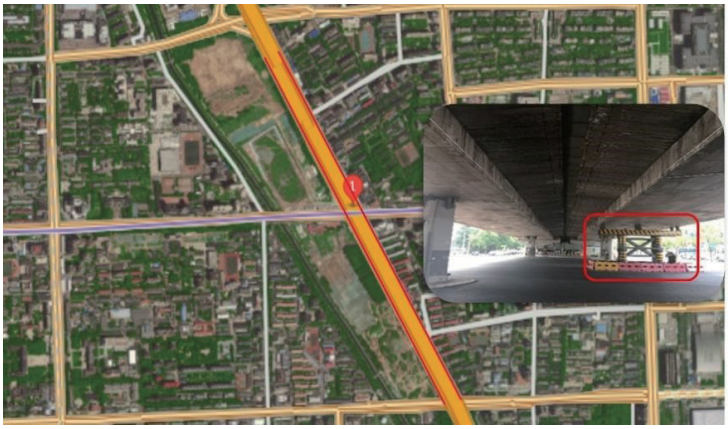

Fig. 7. (Color online) Beishatan Bridge located in Beijing, China.

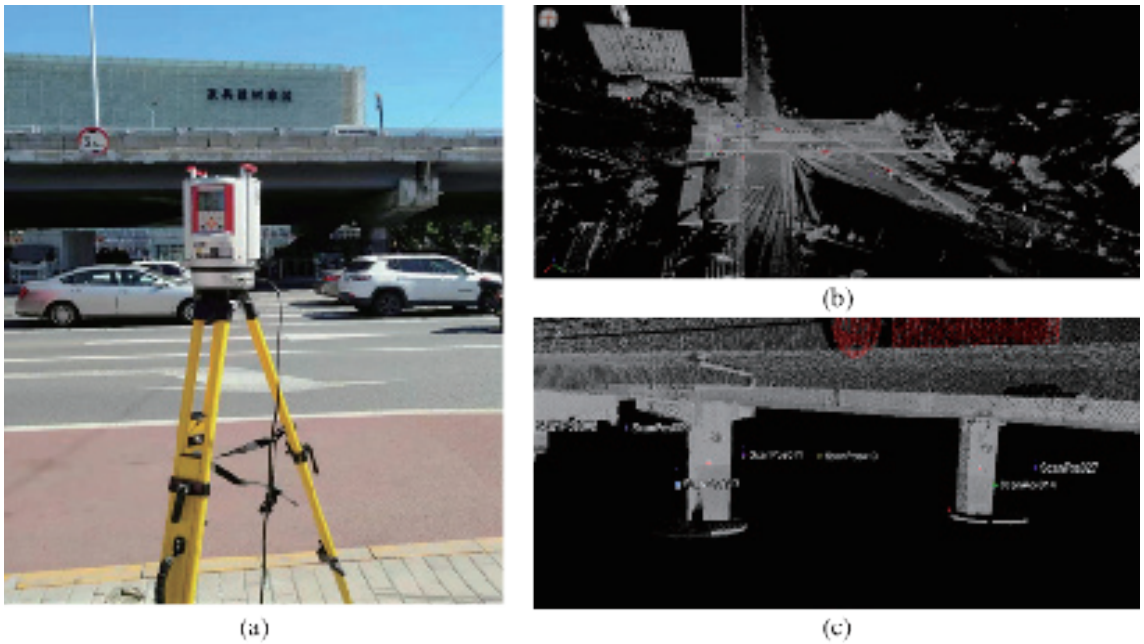

Fig. 8. (Color online) Point cloud acquisition and preprocessing: (a) data acquisition with Riegl VZ-1000, (b) unprocessed point cloud, and (c) preprocessed point cloud.

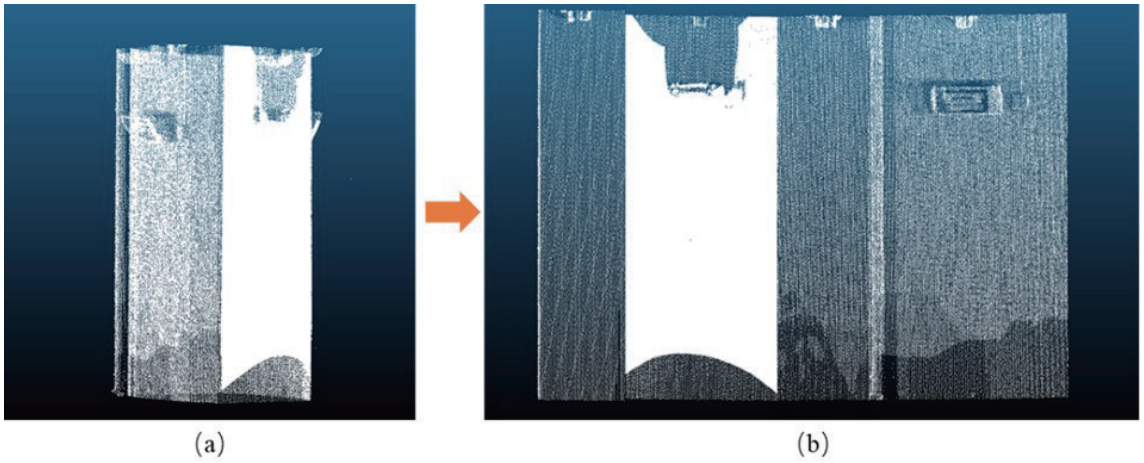

Fig. 9. (Color online) Matrix transformation is applied to unfold the point cloud on the bridge pier outer surface: (a) bridge pier outer surface point cloud and (b) the unfolding of the nonuniform point cloud.

The unfolding of the nonuniform point cloud through matrix transformation is shown in Fig. 9(b). However, the nonuniformity of the point cloud results in low accuracy within the neighborhood range used for curvature calculation. To improve the accuracy of curvature calculation, interpolation is applied using the interpolation method shown in Fig. 10.

Figure 10(b) shows that the bridge pier point cloud becomes smooth and fully represents the overall structure of the bridge pier after applying the interpolation method.

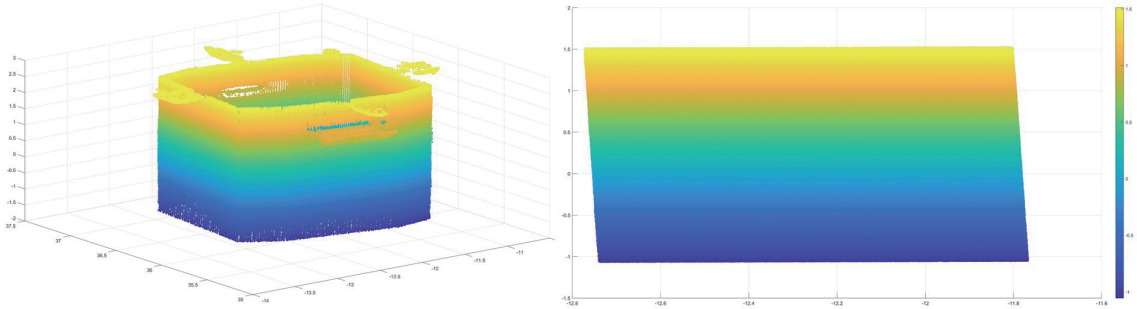

(a) (b)

Fig. 10. (Color online) Interpolation method used to homogenize the bridge pier point cloud: (a) interpolated bridge pier point cloud and (b) interpolated bridge pier point cloud expansion.

3.3 Bridge pier surface shadow texture area identification and elimination

The bridge pier surface is inevitably damaged and bumped during daily operation, resulting in a missing physical model and a shadow texture area in the point cloud. The shadow texture area reduces the accuracy of bridge pier verticality calculation.

To inhibit the effect of the shaded texture area on the pier verticality extraction, it is necessary to calculate the lateral spread and Gaussian curvatures of the outer surfaces of bridge pier point cloud. After removing the Gaussian curvature outliers, the remaining points are the point cloud data of the standard abutment cylinder, as shown in Fig. 11.

To verify the results of eliminating shadow texture areas, we selected bridge piers that conform to a safe operational state for verticality detection. The selected bridge pier is considered a healthy pier.

Figure 12(a) shows that the shadow texture area is not removed, in which the verticalities of positions 6 and 7 have abnormal fluctuations, which are affected by the shadow texture area. Figure 12(b) shows that after the removal of the shadow texture area, the verticalities of positions 6 and 7 can be seen as normal, indicating that the removal of the shadow texture area can improve the accuracy of bridge pier verticality detection.

3.4 Bridge pier structural damage judgement

After applying the above interpolation-matrix change method and eliminating the shadow texture areas to improve the bridge pier curvature calculation accuracy, the bridge pier verticality was calculated. As shown in Fig. 13, the piers of the Beishatan bridge were numbered to meet the pier sequential observation.

The change in verticality was tested for each pier in turn and the results are shown in Fig. 14. As depicted in Fig. 14, the four bridge piers are represented in Fig. 13. We calculated the verticality of the bridge piers after applying the interpolation-matrix transformation method and eliminating the shadow texture regions.

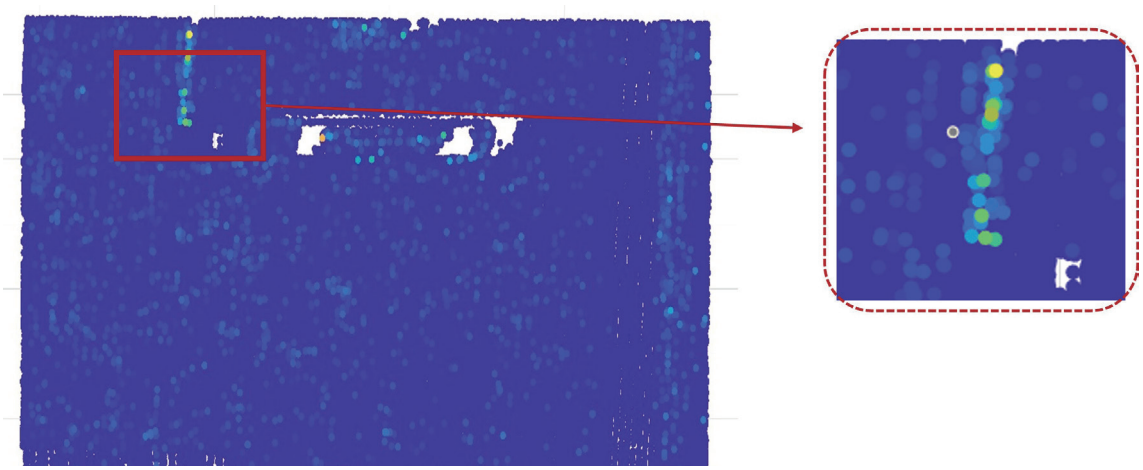

Fig. 11. (Color online) Calculated curvature of the pier outer surface after homogenized unfolding.

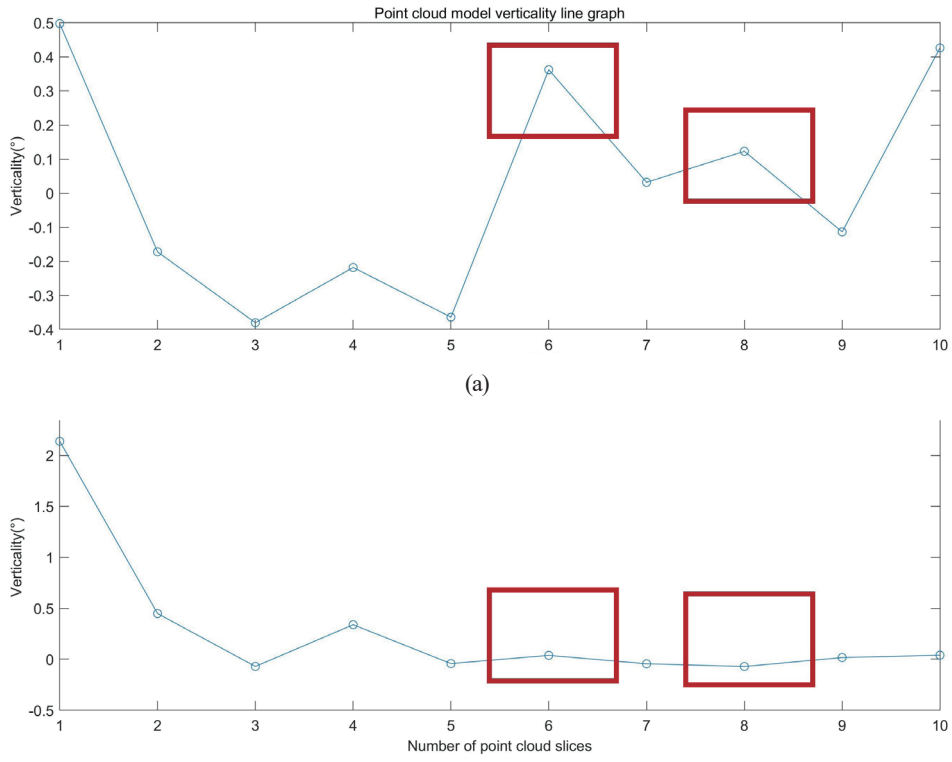

Fig. 12. (Color online) (a) Unshaded shadow texture area and (b) shadow texture area removed.

(1) As shown in Fig. 14, the verticalities of slice positions 1, 2, and 3 of all piers fluctuate considerably. It can be seen through the exploration that the location is the bridge damping region. The range of verticality change in the seismic damping region is large to enhance the pier protection during bridge operation, so the change in slice positions 1, 2, and 3 is not counted in the change in pier verticality.

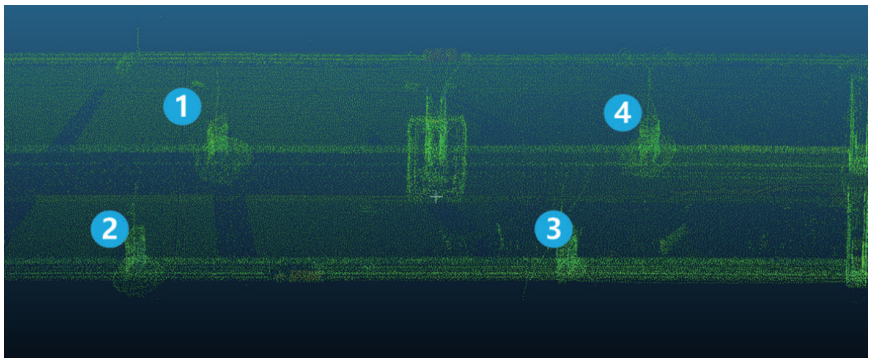

Fig. 13. (Color online) Beishatan bridge pier numbering result.

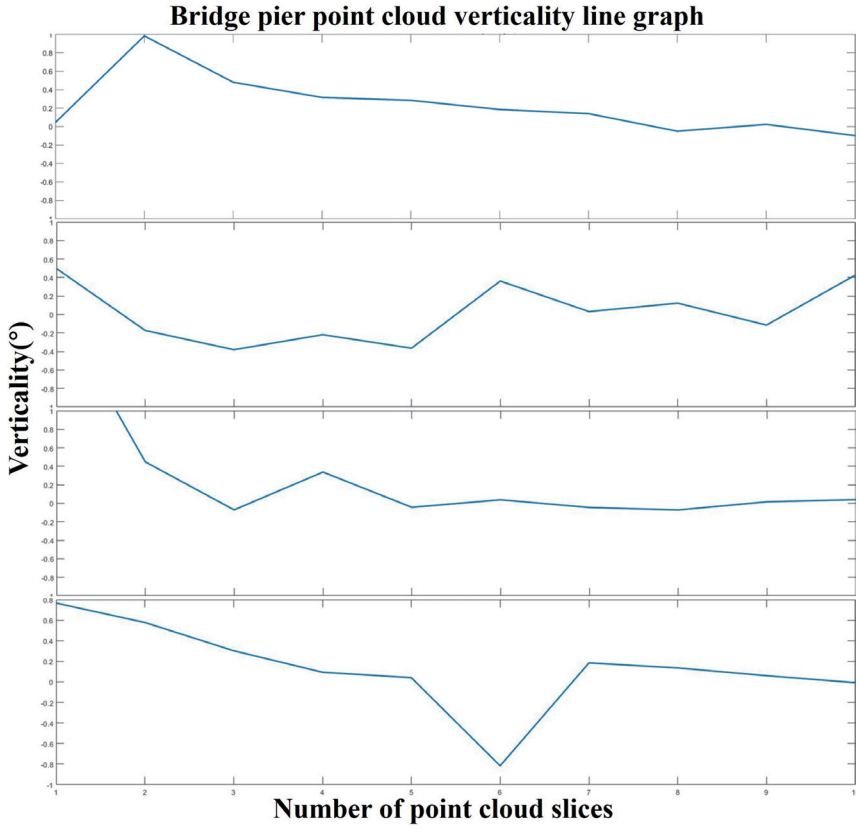

Fig. 14. (Color online) Beishatan bridge pier verticality change.

(2) The height of the bridge pier is 4.5 m. According to national standards, the bridge pier verticality permissible offset range is 1/500 of the pier height. Thus, the degree of offset should be about 0.11°. In Fig. 14, the vertical axis represents the verticality offset. Therefore, it can be found that the bridge pier shown in Fig. 14(d) has been damaged.

4. Conclusions

Bridges are important transportation routes in the process of urbanization. Bridge piers are an important component, and bridge pier damage causes considerable harm to the maintenance of a bridge's daily safe operation. Bridge pier verticality is one of the important indicators of bridge pier damage. Therefore, it is very important to accurately determine the change in bridge pier verticality. The TLS point cloud can be used for complete bridge pier observation. On the basis of the 3D laser point cloud, we proposed a bridge pier point cloud verticality calculation by the interpolation-matrix transformation method and applied it to the detection of the actual damage of a bridge pier. We verified the method's validity, and our research results clearly emphasize the following points:

(1) Changes in bridge pier point cloud verticality can be calculated.
(2) The curvature calculation interpolation-matrix transformation method is proposed, which can eliminate the point cloud nonuniformity problem due to the bridge pier point cloud curvature feature.
(3) We take into account the changes in bridge pier surface curvature characteristics, identify and deal with the shadow areas caused by inevitable damage and bumps during daily operation, improve the bridge pier verticality calculation accuracy, and guarantee the bridge damage detection accuracy based on the changes in bridge pier verticality.

Acknowledgments

This study was supported by the National Natural Science Foundation of China (grant numbers 41871367, 42171416, and 42201488), the National Youth Talent Support Program (grant number SQ2022QB01546), the Joint Project of Beijing Municipal Commission of Education and Beijing Natural Science Foundation (grant number KZ202210016022), the Pyramid Talent Training Project of Beijing University of Civil Engineering and Architecture (grant number JDJQ20220804), the Fundamental Research Funds for Beijing Universities (grant number X20150), the BUCEA Postgraduate Innovation Project, and the Beijing Key Laboratory of Urban Spatial Information Engineering (grant number 20230103).

References

1 M. Pregnolato: Eng. Struct. **196** (2019) 109193. https://doi.org/10.1016/j.engstruct.2019.05.035
2 L. Z. Jiang, X. kang, and L. K. Chen: Eng. Fail. Anal. **140** (2022) 106608. https://doi.org/10.1016/j.engfailanal.2022.106608
3 B. Riveiro, M. J. DeJong, and B. Conde: Autom. Constr. **72** (2016) 258. https://doi.org/10.1016/j.autcon.2016.02.009
4 B. Riveiro, H. González-Jorge, M. Varela, and D. V. Jáuregui: Measurement **46** (2013) 784. https://doi.org/10.1016/j.measurement.2012.09.018
5 P. Palma and R. Steiger: Constr. Build. Mater. **248** (2020) 118528. https://doi.org/10.1016/j.conbuildmat.2020.118528
6 N. Shen, B. Wang, H. Ma, X. Zhao, Y. Zhou, Z. Zhang, and J. Xu: Measurement **223** (2023) 113684. https://doi.org/10.1016/j.measurement.2023.113684
7 B. Riveiro, M. DeJong, and B. Conde: Autom. Constr. **72** (2016) 258. https://doi.org/10.1016/j.autcon.2016.02.009

8 A. Gruen and D. Akca: ISPRS J. Photogramm. Remote Sens. **59** (2005) 151. https://doi.org/10.1016/j.isprsjprs.2005.02.006
9 Z. Zhu, S. German, and I. Brilakis: Autom. Constr. **19** (2010) 1047. https://doi.org/10.1016/j.autcon.2010.07.016
10 H. Hu, Y. Ding, Q. Zhu, B. Wu, H. Lin, Z. Du, and Y. Zhang: ISPRS J. Photogramm. Remote Sens. **92** (2014) 98. https://doi.org/10.1016/j.isprsjprs.2014.02.014
11 G. Morgenthal, N. Hallermann, J. Kersten, J. Taraben, P. Debus, M. Helmrich, and V. Rodehorst: Autom. Constr. **97** (2019) 77. https://doi.org/10.1016/j.autcon.2018.10.006
12 A. Aryal, B. Brooks, M. Reid, G. Bawden, and G. Pawlak: J. Geophys. Res.: Earth Surf. **117** (2012) F1. https://doi.org/10.1029/2011JF002161
13 L. Truong-Hong and R. Lindenbergh: Autom. Constr. **135** (2022) 104127. https://doi.org/10.1016/j.autcon.2021.104127
14 Y. Deng, C. Yan, S. Liu, J. Wang, Z. Sun, and K. Cui: Eng. Struct. **258** (2022) 114106. https://doi.org/10.1016/j.engstruct.2022.114106
15 F. A. Limberger and M. M. Oliveira: Pattern Recognit. **48** (2015) 2043. https://doi.org/10.1016/j.patcog.2014.12.020
16 N. Saovana, N. Yabuki, and T. Fukuda: Autom. Constr. **129** (2021) 103804. https://doi.org/10.1016/j.autcon.2021.103804
17 N. Kassotakis and V. Sarhosis: Structures **32** (2021) 1777. https://doi.org/10.1016/j.istruc.2021.03.111
18 L. Truong-Hong and R. Lindenbergh: Autom. Constr. **135** (2022) 104127. https://doi.org/10.1016/j.autcon.2021.104127
19 X. Yang, E. R. Castillo, Y Zou, L. Wotherspoon, and Y. Tan: Autom. Constr. **142** (2022) 104519. https://doi.org/10.1016/j.autcon.2022.104519
20 C. Koch, K. Georgieva, V. Kasireddy, B. Akinci, and P. Fieguth: Adv. Eng. Inf. **29** (2015) 196. https://doi.org/10.1016/j.aei.2015.01.008
21 X. Deng, S. Wang, Y. Zhuang, Y. Fan, and Y. Zhou: J. Eng. Appl. Sci. **70** (2023) 135. https://doi.org/10.1186/s44147-023-00308-3
22 B. Zhu, Y. Ye, L. Zhou, Z. Li, and G. Yin: ISPRS J. Photogramm. Remote Sens. **181** (2021) 129. https://doi.org/10.1016/j.isprsjprs.2021.09.010
23 M. Omer, L. Margetts, M. Mosleh, and L. Cunningham: J. Bridge Eng. **26** (2021) 05021010. https://doi.org/10.1061/(ASCE)BE.1943-5592.0001759
24 I. H. Kim, H. Jeon, S. C. Baek, W. H. Hong, and H. J. Jung: Sensors **18** (2018) 1881. https://doi.org/10.3390/s18061881
25 B. Butchibabu, N. Sandeep, Y. V. Sivaram, P. C. Jha, and P. K. Khan: J. Appl. Geophys. **144** (2017) 104. https://doi.org/10.1016/j.jappgeo.2017.07.008